

Transverse momentum parton distributions inspired by a quark potential model

F.K. Diakonou, G.D. Galanopoulos and X.N. Maintas

Department of Physics, University of Athens, GR-15771 Athens, Greece

Abstract

We derive a nonperturbative transverse momentum distribution for partons using a potential model to describe the quark-quark interaction inside the proton. We use this distribution to calculate the differential cross-section of π^0 -production for intermediate values of transverse momentum in $p - p$ collisions at high energies. Assuming a variable string tension constant for the quark-quark potential we obtain a very good description of the experimental data at different energies. The corresponding values of the mean transverse momentum of the partons are essentially lower than those obtained using a Gaussian transverse momentum parton distribution.

1 Introduction

During the last decades the tests of the perturbative QCD are focused on the experimental [1-15] and theoretical study [16-26] of hard processes like direct photon and π^0 -production with large transverse momentum in pp , pA and AA collisions. These processes offer a unique possibility to determine

the parton distribution functions (PDF) inside the proton as well as the parton fragmentation functions (PFF). In particular the good understanding of the pp data is the prerequisite for any attempt to extract new physics, related to the formation of a quark-gluon plasma phase, from the pA and AA data. Extensive studies of the π (or γ) production in pp collisions have shown that the transverse momentum distribution $g(k_T)$ of the partons inside the proton has to be taken into account for a successful description of the observed p_T spectrum [20-23]. In all these investigations one assumes a Gaussian form for $g(k_T)$. A new nonperturbative parameter is introduced through this approach: the mean intrinsic transverse momentum $\langle k_T \rangle$ of the partons. Although the data of some experiments concerning hadron production at large p_T [20, 21] could be explained with relative small $\langle k_T \rangle$ values ($\approx 0.3 - 0.5 \text{ GeV}$), compatible with the Heisenberg uncertainty relation for partons inside the proton, there are a number of other processes leading to a large mean transverse momentum ($\langle k_T \rangle \approx 1 - 4 \text{ GeV}$), depending on Q^2 , for a description of the corresponding experimental data. Such a value of $\langle k_T \rangle$ is too high and cannot be explained as an internal structure of the proton [23]. However, as mentioned by several authors [19, 21] the form of $g(k_T)$ can influence significantly the value of $\langle k_T \rangle$ as well as its p_T dependence. In the present work we derive a transverse momentum distribution for the partons inside the proton using a potential quark model which has successfully been used to describe the spectra of mesonic [27] and baryonic [28] bound states in the past. Following [28, 29] we investigate the three-body quantum mechanical bound state problem solving numerically the Schrödinger equation and obtaining the single particle transverse momentum distribution for the constituent parton. Our main assumption is that intrinsic transverse momentum effects are not influenced by the Lorentz boost along the beam axis and therefore could be treated within a nonrelativistic approach. We use the derived distribution to fit experimental data for the $pp \rightarrow \pi_0 + X$ process. In particular we investigate the measurements for the p_T -spectrum of the outgoing π^0 in three experiments performed at different center of mass energies. It turns out that a relatively low mean transverse momentum $\langle k_T \rangle$ ($\approx O(300 \text{ MeV})$), compatible with intrinsic dynamics inside the proton, for the initial partons is sufficient in order to fit perfectly the experimental data. A smooth dependence of $\langle k_T \rangle$ on p_T , which within our approach is induced by a corresponding variation of the string tension in the quark-quark potential, is required. Our analysis shows that the k_T distribution of the constituent partons can be strongly influenced

by three-body effects and the form of the confining potential which have to be taken into account in order to describe correctly the experimental data concerning the pion production in pp collisions. The paper is organized as follows: in Section 2 we present the parton model differential cross section as well as the corresponding kinematics for the π^0 -production in pp -collisions. In section 3 we derive the intrinsic transverse momentum distribution for the partons inside the proton using the quark potential model of [27]. In section 4 we present our numerical results concerning the description of the data of three different experiments [1, 6, 15] as well as the corresponding dependence $\langle k_T(p_T) \rangle$. Finally in section 5 we summarize our study and we discuss possible extensions of the present analysis.

2 The $pp \rightarrow \pi^0 + X$ cross section

In the lowest-order perturbative QCD (pQCD), the differential cross section for the direct pion production in pp collisions is given by:

$$E_\pi \frac{d\sigma}{d^3p}(pp \rightarrow \pi^0 + X) = K \sum_{abcd} \int dx_a dx_b f_{a/p}(x_a, Q^2) f_{b/p}(x_b, Q^2) \times \frac{d\sigma}{d\hat{t}}(ab \rightarrow cd) \frac{D_{\pi/c}(z_c, Q^2)}{\pi z_c} \quad (1)$$

where $f_{i/p}$ ($i = a, b$) are the longitudinal parton distribution functions (PDF) for the colliding partons a and b while $D_{\pi/c}$ is the parton fragmentation function (PFF) for the pion. For the scale Q we use the relation $Q^2 = \frac{2\hat{s}\hat{t}\hat{u}}{\hat{s}^2 + \hat{t}^2 + \hat{u}^2}$ proposed in [19] with \hat{s} , \hat{t} , \hat{u} the usual Mandelstam variables. The variable z_c indicates the momentum fraction carried by the final hadron. The higher order corrections are taken into account by choosing $K \approx 2$ for the corresponding coefficient in (1) in the p_T region of interest. It is straightforward to include partonic transverse degrees of freedom using the following replacement [21] in the PDFs of eq.(1):

$$dx_i f_{i/p}(x_i, Q^2) \longrightarrow dx_i d^2k_{T,i} g(\vec{k}_{T,i}) f_{i/p}(x_i, Q^2) \quad (2)$$

with $i = a, b$. In order to avoid singularities in the differential cross sections describing the partonic subprocesses we introduce a regularizing parton mass $m = 0.8 \text{ GeV}$, as in [19], in the Mandelstam variables occurring in the denominator of the corresponding matrix elements. The explicit formulas of the

relevant partonic cross sections can be found in [21]. Taking into account the transverse degrees of freedom we get the following expressions for the variables \hat{s} , \hat{t} , \hat{u} :

$$\begin{aligned}\hat{s} &= sx_a x_b + \frac{k_{T,a}^2 k_{T,b}^2}{sx_a x_b} - 2\vec{k}_{T,a} \cdot \vec{k}_{T,b} \\ \hat{t} &= -(x_a + \frac{k_{T,a}^2}{sx_a}) \frac{p_T \sqrt{s}}{z_c} + \frac{2}{z_c} \vec{k}_{T,a} \cdot \vec{p}_T \\ \hat{u} &= -(x_b + \frac{k_{T,b}^2}{sx_b}) \frac{p_T \sqrt{s}}{z_c} + \frac{2}{z_c} \vec{k}_{T,b} \cdot \vec{p}_T\end{aligned}\tag{3}$$

Due to energy-momentum conservation the momentum fraction of the final hadron z_c is given by:

$$z_c = \frac{(x_a + \frac{k_{T,a}^2}{sx_a} + x_b + \frac{k_{T,b}^2}{sx_b}) p_T \sqrt{s} - 2(\vec{k}_{T,a} + \vec{k}_{T,b}) \cdot \vec{p}_T}{\hat{s}}\tag{4}$$

For a consistent description of the kinematics in the partonic subprocesses we imply the cuts:

$$z_c \leq 1 \quad ; \quad k_{T,a}^2 < p_T \sqrt{s} \quad ; \quad k_{T,b}^2 < p_T \sqrt{s}\tag{5}$$

To calculate the cross section given in eq.(1) we have first to determine the distribution $g(\vec{k}_T)$ and then perform the corresponding phase space integrations. Contrary to the usual treatment assuming a Gaussian form for $g(\vec{k}_T)$ we will here derive an alternative expression based on a widely applied quark potential model.

3 The intrinsic transverse momentum distribution $g(\vec{k}_T)$

Since the early days of quantum chromodynamics the main and almost unique tool used for the description of the hadronic bound states (mesons, baryons) remain potential models for the quark-quark and quark-antiquark pair interaction. One of the most succesfull models was proposed by A. Martin used first to describe mesonic states [27] and later to describe baryons [28]. The quark-quark interaction within this model is given as:

$$V(r) = A_{qq} r^{0.1} + B_{qq}\tag{6}$$

and a similar expression with adapted coefficients $A_{\bar{q}q}$, $B_{\bar{q}q}$ holds for the quark-antiquark interaction. In the following we will consider a baryon consisting of 3 valence quarks interacting pairwise with the potential (6). The Hamiltonian operator of the system is given as:

$$\hat{H} = -\frac{\hbar^2}{2m}(\nabla_1^2 + \nabla_2^2 + \nabla_3^2) + V(\vec{r}_{12}) + V(\vec{r}_{23}) + V(\vec{r}_{31}) \quad (7)$$

The baryonic ground state can then be obtained by solving the corresponding Schrödinger equation. Following [28] it is convenient to introduce Jacobi coordinates $\vec{\xi}_i$:

$$\begin{aligned} \vec{\xi}_1 &= \vec{r}_2 - \vec{r}_1 \\ \vec{\xi}_2 &= \frac{2\vec{r}_3 - \vec{r}_2 - \vec{r}_1}{\sqrt{3}} \\ \vec{\xi}_3 &= \frac{\vec{r}_1 + \vec{r}_2 + \vec{r}_3}{3} \end{aligned} \quad (8)$$

getting the equation:

$$\left[-\frac{\hbar^2}{2M}\vec{\nabla}_{\xi_3}^2 - \frac{\hbar^2}{m}(\vec{\nabla}_{\xi_1}^2 + \vec{\nabla}_{\xi_2}^2) + \tilde{V}(\vec{\xi}_1, \vec{\xi}_2) \right] \Psi_G(\vec{\xi}_1, \vec{\xi}_2, \vec{\xi}_3) = E_G \Psi_G(\vec{\xi}_1, \vec{\xi}_2, \vec{\xi}_3) \quad (9)$$

with $M = 3m$ and m is the constituent quark mass. Eliminating the translational mode ($\vec{\xi}_3$) we obtain a partial differential equation (PDE) depending solely on the variables $\vec{\xi}_1, \vec{\xi}_2$. The potential energy \tilde{V} in eq.(9) is given as:

$$\tilde{V}(\vec{\xi}_1, \vec{\xi}_2) = V(\vec{\xi}_1) + V\left(\frac{1}{2}(\vec{\xi}_1 - \sqrt{3}\vec{\xi}_2)\right) + V\left(\frac{1}{2}(\sqrt{3}\vec{\xi}_2 + \vec{\xi}_1)\right) \quad (10)$$

Introducing the radial variable $\xi = \sqrt{\xi_1^2 + \xi_2^2}$ and the angular variables $\chi, \theta_1, \phi_1, \theta_2, \phi_2$ we rewrite eq.(9) as follows:

$$\begin{aligned} -\frac{\hbar^2}{m}\left\{\frac{1}{\xi^5}\partial_\xi\left(\xi^5\partial_\xi\tilde{\Psi}\right) + \frac{1}{\xi^2}\left[\frac{1}{\sin^2 2\chi}\partial_\chi\left(\sin^2 2\chi\partial_\chi\tilde{\Psi}\right) + \frac{\hat{L}_1^2\tilde{\Psi}}{\cos^2 \chi} + \frac{\hat{L}_2^2\tilde{\Psi}}{\sin^2 \chi}\right]\right\} \\ + \tilde{V}(\xi, \chi, \theta_1, \phi_1, \theta_2, \phi_2)\tilde{\Psi} = E_G \tilde{\Psi} \end{aligned} \quad (11)$$

where the angular momentum operators are:

$$\hat{L}_i^2 = -\left[\frac{1}{\sin \theta_i}\frac{\partial}{\partial \theta_i}\left(\sin \theta_i\frac{\partial}{\partial \theta_i}\right) + \frac{1}{\sin^2 \theta_i}\frac{\partial^2}{\partial \phi_i^2}\right]$$

The reduced ground state wave function $\tilde{\Psi}$ can be expressed in terms of the hyperspherical harmonics $P_L(\Omega)$ as follows:

$$\tilde{\Psi}(\xi, \chi, \theta_1, \phi_1, \theta_2, \phi_2) = \sum_{L=0}^{\infty} \frac{u_L(\xi)}{\xi^{5/2}} P_L(\chi, \theta_1, \phi_1, \theta_2, \phi_2) \quad (12)$$

The radial part of the wave function $\tilde{\Psi}$ fullfils the equation [29]:

$$\frac{d^2 u_L}{d\xi^2} - \frac{15/4 + L(L+4)}{\xi^2} u_L + \frac{m}{\hbar^2} E_G u_L - \frac{m}{\hbar^2} \sum_{L'} u_{L'} \tilde{V}_{LL'} = 0 \quad (13)$$

As mentioned in [28] the matrix $\tilde{V}_{LL'} = \int d\Omega P_L^*(\Omega) \tilde{V}(\xi, \Omega) P_{L'}(\Omega)$ for the particular choise of the potential (6) is diagonal dominant and therefore to a very good approximation the ground state of the baryonic system is determined by the $L = 0$ term in the expansion (12). Therefore the radial part of the ground state wavefunction obeys, within the above approximation, the equation:

$$\frac{d^2 u_0}{d\xi^2} - \frac{15}{4\xi^2} u_0 + \frac{m}{\hbar^2} (E_G - \tilde{V}_{00}) u_0 = 0 \quad (14)$$

where: $\tilde{V}_{00} = A_{00} + B_{00}\xi^{0.1}$ with $A_{00} = \frac{3}{2}A_{qq}$ and $B_{00} = \frac{1}{2}\lambda B_{qq}$. The constant λ is given by: $\lambda = \frac{24}{\pi}\Gamma(1.55)\Gamma(1.5)\Gamma(3.05)$. It is straightforward to show that the ground state wavefunction in the momentum space (conjugate to the space of $\vec{\xi}_i$, $i = 1, 2, 3$) is given by:

$$\tilde{\Phi}(k_\xi^2) = N \int_0^\infty d\xi \xi^{1/2} u_0(\xi) \frac{J_2(k_\xi \xi) - k_\xi \xi J_3(k_\xi \xi)}{k_\xi^2} \quad (15)$$

where J_n is the Bessel function of order n and N is a normalization constant. It is useful to determine the transformation of the momenta \vec{k}_{ξ_i} to the cartesian momenta \vec{k}_i :

$$\begin{aligned} \vec{k}_{\xi_1} &= -\frac{1}{2}(\vec{k}_1 - \vec{k}_2) \\ \vec{k}_{\xi_2} &= -\frac{1}{2\sqrt{3}}(\vec{k}_1 + \vec{k}_2 - 2\vec{k}_3) \\ \vec{k}_{\xi_3} &= \frac{1}{\sqrt{3}}(\vec{k}_1 + \vec{k}_2 + \vec{k}_3) \end{aligned} \quad (16)$$

The above expressions simplify in the center of mass frame $\vec{k}_{\xi_3} = \vec{0}$ of the baryonic system where the following relation is valid:

$$k_\xi^2 = k_1^2 + k_2^2 + \vec{k}_1 \cdot \vec{k}_2$$

The two-particle density $\rho(\vec{k}_1, \vec{k}_2)$ in this case is given by:

$$\rho(\vec{k}_1, \vec{k}_2) = |\tilde{\Phi}(k_\xi^2)|^2 = |\tilde{\Phi}(k_1^2 + k_2^2 + \vec{k}_1 \cdot \vec{k}_2)|^2 \quad (17)$$

From eq.(17) we obtain the one-particle transverse momentum density $g(\vec{k}_T)$ as:

$$g(\vec{k}_T) = 4\pi \int_0^\infty dk_z \int_{-1}^1 dz \int_0^\infty dk_2 k_2^2 |\tilde{\Phi}(k_T^2 + k_z^2 + k_2^2 + z k_2 \sqrt{k_T^2 + k_z^2})|^2 \quad (18)$$

where z is the cosine of the angle between the vectors $\vec{k} = (\vec{k}_T, k_z)$ and \vec{k}_2 . In fact the function $u_0(\xi)$ can be obtained only numerically by solving equation (14) using the Numerov algorithm. Therefore also the transverse momentum distribution (18) is known only numerically. The integrations in eqs.(15,18) can be performed to a great accuracy (relative error $\approx 10^{-6}$) using a mixture of Gauss-Kronrod quadrature and the VEGAS Monte-Carlo integration routine [30]. In Fig. 1 we present the density in transverse momentum space of a parton inside the proton obtained by our approach. The values of the constants A_{qq} and B_{qq} are chosen according to [28] in order to fit the size and the binding energy of the proton. The characteristic structure dominating the form of $g(\vec{k}_T)$ within our model is the second maximum at relative high transverse momenta. This leads, as we will see in the next section, to a reduction, relative to the Gaussian case, of the mean intrinsic transverse momentum of the partons needed to describe the experimental data for the π^0 -production at various energies.

4 Numerical results

In the following we will use the derived distribution $g(\vec{k}_T)$ in order to calculate within the parton model the differential cross section for the π^0 -production in pp collisions according to eq.(1). For the longitudinal parton distribution functions we use the recent Martin, Roberts, Stirling and Thorne (MRST) scheme [31] while for the parton fragmentation functions we use the Kniehl, Kramer, Potter [32] parametrization. The additional nonperturbative parameter in our treatment is the mean value of the intrinsic transverse momentum $\langle k_T \rangle$ which is related to the string tension B_{qq} in eq.(6). Although the distribution $g(\vec{k}_T)$ is derived for the valence quarks inside the proton here we will use the same distribution also for the initial gluons assuming universality at the level of constituent partons. In any case for longitudinal

momentum fraction $x_i > 0.5$ ($i = a, b$) the contribution of valence quarks is dominant and our description is accurate. The phase space integrations are performed using the VEGAS Monte-Carlo routine. In order to fit the experimental data we allow $\langle k_T \rangle$ to vary as a function of the beam energy and the transverse momentum (p_T) of the finally produced hadron. We will analyse here the results of three experiments concerning π^0 -production at different energies. The first set of data are taken from the fixed target experiment performed in Fermilab (protons incident on H_2 target) [1]. The cross section for the π^0 -production with transverse momentum p_T at midrapidity and for three different proton beam energies $E_L = 200, 300$ and 400 GeV is measured. In Fig. 2 we present the various datasets using symbols while with solid lines we show the results of our calculation and with dashed lines the corresponding results using a Gaussian $g(\vec{k}_T)$. As we can see the two descriptions differ only in the region $p_T < 1$ GeV . Within our approach we need an intrinsic transverse momentum $\langle k_T \rangle$ of the order of at most 0.5 GeV in order to reproduce all the experimental data. It must be noted that in this case one can perfectly fit the data also for $p_T < 1$ GeV which, as we see in Fig. 2, is not possible using a Gaussian distribution $g(\vec{k}_T)$. In Fig. 3 we show the functions $\langle k_T \rangle(p_T)$ obtained using the quark model inspired function $g(\vec{k}_T)$ as well as a Gaussian form. It is evident that the Gaussian model leads to much higher values of $\langle k_T \rangle$. In particular this difference is large even for large values of p_T where our approach is more precise as the valence quark contribution is dominant. As already discussed in the previous section this difference relies on the fact that the non-Gaussian $g(\vec{k}_T)$ derived here possesses a second small local maximum at high transverse momenta (see Fig. 1) attributed to the form of the quark-quark potential and the many-body character of the system.

The second experiment we consider is the WA70 at CERN SPS [6]. It is also a fixed target experiment with $E_L = 280$ GeV . We are interested in π^0 -production. In Fig. 4 we show the experimental data (full stars) and the corresponding pQCD calculation using the quark model inspired $g(\vec{k}_T)$ (solid line) as well as a Gaussian form (dashed line). Both distributions reproduce perfectly the experimental data and cannot be distinguished graphically. However our approach leads to significantly lower values of $\langle k_T \rangle$ than in the Gaussian case. This can be clearly seen in Fig. 5 where we show the function $\langle k_T(p_T) \rangle$ both for the quark potential model inspired $g(\vec{k}_T)$ (full circles) as well as the Gaussian intrinsic transverse momentum distribu-

tion (full stars). Also in this case the difference in $\langle k_T \rangle$ between the two approaches is large in a p_T -region where the main contribution is attributed to the valence quarks. For comparison we present also the same function for the Fermilab experiment at $E_L = 300 \text{ GeV}$ (open circles, see Fig. 3).

Finally we have analysed the $pp \rightarrow \pi^0 + X$ data of the most recent PHENIX experiment at the Relativistic Heavy Ion Collider with $\sqrt{s} = 200 \text{ GeV}$ [15]. The corresponding cross section can be described to a good accuracy without inclusion of any k_T -smearing, a fact which is compatible with expectations for the perturbative character of the subprocesses involved in this case. Here we have fitted the experimental data using non-Gaussian k_T -smearing effects. In this way we get a perfect description of the measured cross section. The obtained mean intrinsic transverse momentum is almost constant: $\langle k_T \rangle \approx 250 \text{ MeV}$. Based on Heisenberg uncertainty relation one could explain this value of the mean transverse momentum as an effect of the internal partonic structure of the incident proton. Our results are presented in Figs. 6,7. The PHENIX data (open circles) for $E \frac{d^3\sigma}{dp^3}$ together with the parton model calculations (crosses) using non-Gaussian $g(\vec{k}_T)$ are shown in Fig. 6. The corresponding function $\langle k_T \rangle(p_T)$ is presented in Fig. 7.

5 Concluding remarks

Using a quark potential model capable to describe consistently baryonic systems as three quark bound states we have derived an intrinsic transverse momentum distribution $g(\vec{k}_T)$ of partons inside the proton. This, clearly non-Gaussian, distribution is characterized by the presence of a smooth local maximum at relatively high transverse momenta. Our approach is based on the idea that transverse momentum effects may be described nonrelativistically as they are not influenced by the Lorentz boost along the beam axis. Describing the k_T -smearing effects in the parton model for pp collisions through this non-Gaussian distribution we calculated the differential cross section for π^0 -production at midrapidity for different beam energies. Assuming that the corresponding nonperturbative parameter $\langle k_T \rangle$, related to $g(\vec{k}_T)$, depends on p_T of the finally produced hadron as well as the incident energy, we obtain a perfect description of the experimental data measured in pp collisions at three different experiments. The corresponding values of $\langle k_T \rangle$ as a function of p_T could originate, according to Heisenberg uncertainty relation, from the internal partonic structure of the proton. Our approach is expected to be

valid also in single photon production as well as pA and AA processes [33]. Therefore the performed analysis shows that many-body effects through a confining potential, reflected at the level of one-particle distributions, may influence strongly the k_T -smearing phenomena observed in hadronic collisions and therefore should be taken into account for a correct description of the experimental data.

Acknowledgment We thank N.G. Antoniou for helpful discussions. This work is financed by EPEAEK in the framework of PYTHAGORAS grants supporting University research groups under contract 70/3/7420.

References

- [1] CP Collaboration, D. Antreasyan *et al.*, Phys. Rev. **D19**, 764 (1979).
- [2] E704 Collaboration, D.L. Adams *et al.*, Phys. Lett. **B345**, 569 (1995); Phys. Rev. **D53**, 4747 (1996).
- [3] NA24 Collaboration, C. De Marzo *et al.*, Phys. Rev. **D36**, 16 (1987).
- [4] R110 Collaboration, A.L.S. Angelis *et al.*, Phys. Lett. **B185**, 213 (1987).
- [5] E605 Collaboration, D.E. Jaffe *et al.*, Phys. Rev. **D40**, 2777 (1989).
- [6] WA70 Collaboration, M. Bonesini *et al.*, Z. Phys. **C38**, 371 (1988).
- [7] R807/AFS Collaboration, T. Akesson *et al.*, Yad. Fiz. **51**, 1314 (1990) [Sov. J. Nucl. Phys. **51**, 836 (1990)].
- [8] UA6 Collaboration, G. Balocchi *et al.*, Phys. Lett. **B436**, 222 (1998).
- [9] R108 Collaboration, A.L.S. Angelis *et al.*, Phys. Lett. **B94**, 106 (1980).
- [10] R110 Collaboration, A.L.S. Angelis *et al.*, Nucl. Phys. **B327**, 541 (1989).
- [11] R108 Collaboration, E. Anassontzis *et al.*, Z. Phys. **C13**, 277 (1982).
- [12] E772 Collaboration, D.M. Alde *et al.*, Phys. Rev. Lett. **64**, 2479 (1990).

- [13] E866 Collaboration, M.J. Leitch *et al.*, nucl-ex/9909007.
- [14] E706 Collaboration, L. Apanasevich *et al.*, Phys. Rev. Lett. **81**, 2642 (1998); Phys. Rev. **D59**, 074007 (1999).
- [15] PHENIX Collaboration, S.S. Adler *et al.*, Phys. Rev. Lett. **91**, 241803 (2003).
- [16] R.D. Field, *Applications of Perturbative QCD*, Frontiers in Physics Lecture, Vol. 77 (Addison-Wesley, Reading, MA, 1989).
- [17] J. Huston, E. Kovacs, S. Kuhlmann, H.L. Lai, J.F. Owens, and W.K. Tung, Phys. Rev. **D51**, 6139 (1995).
- [18] M. Zielinski, hep-ph/9811278.
- [19] R.P. Feynman, R.D. Field and G.C. Fox, Phys. Rev. **D18**, 3320 (1978).
- [20] D. Sivers, S. Brodsky, and R. Blankenbecler, Phys. Rep., Phys. Lett. **23C**, 1 (1976); A.P. Contogouris, R. Gaskell, and S. Papadopoulos, Phys. Rev. **D17**, 2314 (1978).
- [21] J.F. Owens, Rev. Mod. Phys. **59**, 465 (1987).
- [22] X.N. Wang, Phys. Rep. **208**, 287 (1997); Phys. Rev. Lett. **81**, 2655 (1998); Phys. Rev. **C58**, 2321 (1998).
- [23] Y. Zhang, G. Fai, G. Papp, G.G. Barnaföldi, and P. Lévai, Phys. Rev. **C65**, 034903 (2002).
- [24] X. Guo and J. Qiu, Phys. Rev. **D53**, 6144 (1996).
- [25] H.L. Lai and H.N. Li, Phys. Rev. **D58**, 114020 (1998).
- [26] G. Papp, P. Lévai, and G. Fai, Phys. Rev. **C61**, 021902(R).
- [27] A. Martin, Phys. Lett. **B100**, 511 (1981).
- [28] J.M. Richard, Phys. Lett. **B100**, 515 (1981).
- [29] E. Cuervo-Reyes, M. Rigol, and J. Rubayo-Soneira, Revista Brasileira de Ensino de Física, **25**, 18 (2003).

- [30] G.P. Lepage, J. Comput. Phys. **27**, 192 (1978).
- [31] A.D. Martin, R.G. Roberts, W.J. Stirling, and R.S. Thorne, hep-ph/0410230.
- [32] B.A. Kniehl, G. Kramer, B. Potter, Nucl. Phys. **B582**, 514 (2000).
- [33] F.K. Diakonov, N. Kaplis, X.N. Maintas, and C. Papoulias, in preparation.

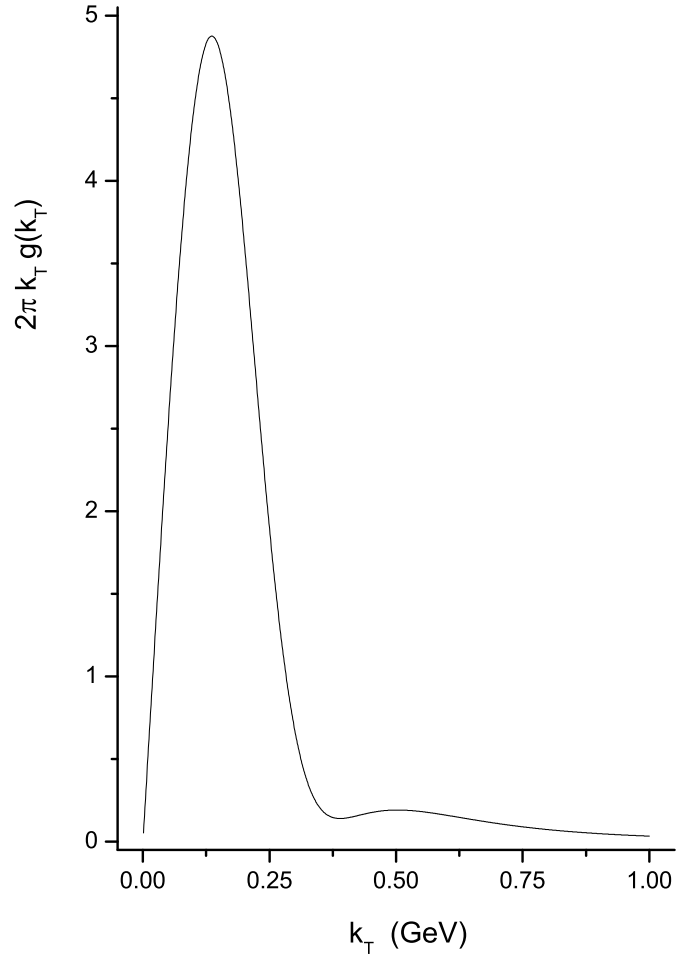


Figure 1: The intrinsic transverse momentum distribution $2\pi k_T g(\vec{k}_T)$ of a parton inside the proton obtained through the quark potential model described in section II.

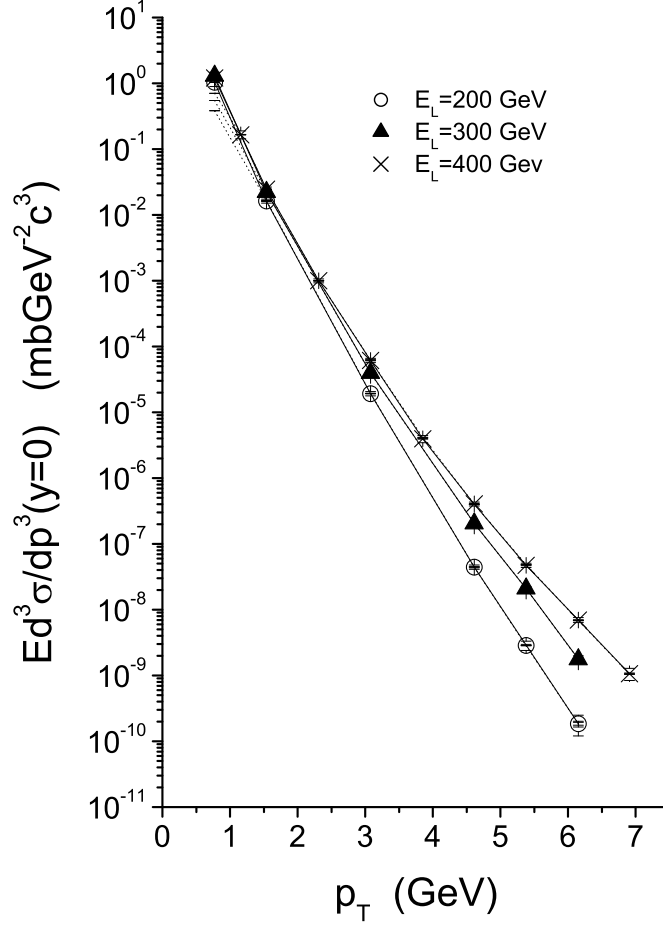


Figure 2: The differential cross section for the π^0 -production in the Fermilab experiment [1]. The symbols represent the experimental datasets for three different beam energies. The solid lines represent the parton model results using a non-Gaussian $g(\vec{k}_T)$ while the dotted lines correspond to the analogous results using a Gaussian k_T -smearing. Only for $p_T < 1 \text{ GeV}$ the two fits differ.

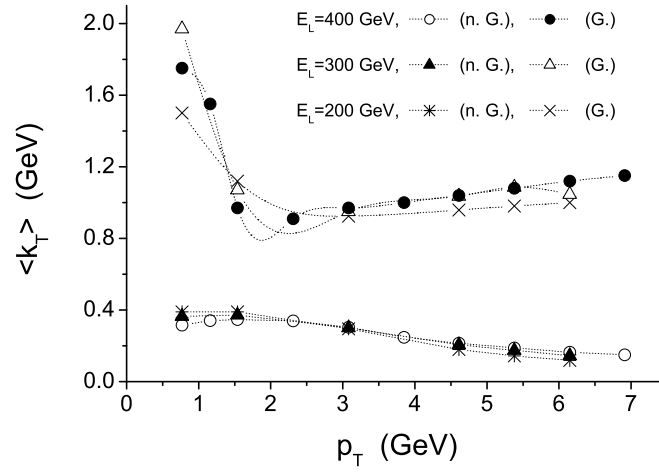


Figure 3: The functions $\langle k_T(p_T) \rangle$ for the three datasets presented in Fig. 2. We distinguish between the results of the parton model using non-Gaussian (n. G.) or Gaussian (G.) intrinsic transverse momentum distribution.

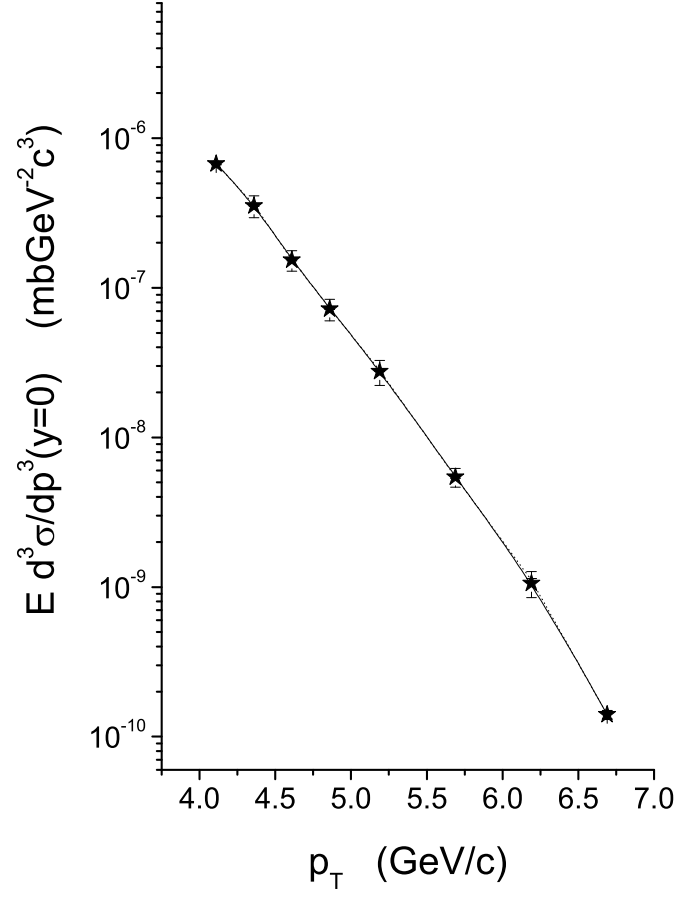


Figure 4: The differential cross section for π^0 -production in WA70 at $E_L = 280$ GeV (full stars) and the corresponding parton model calculation using a non-Gaussian (solid line) as well as a Gaussian (dotted line) $g(\vec{k}_T)$.

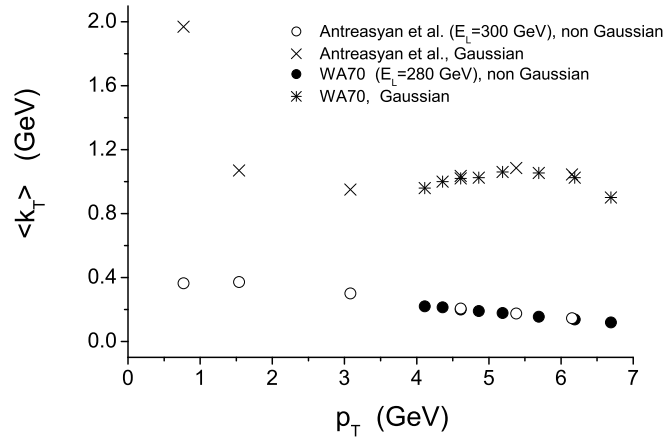


Figure 5: The dependence $k_T(p_T)$ for the WA70 data set using a non-Gaussian as well as a Gaussian $g(\vec{k}_T)$ in comparison with the corresponding behaviour found for the Fermilab experiment at $E_L = 300$ GeV with a non-Gaussian $g(\vec{k}_T)$.

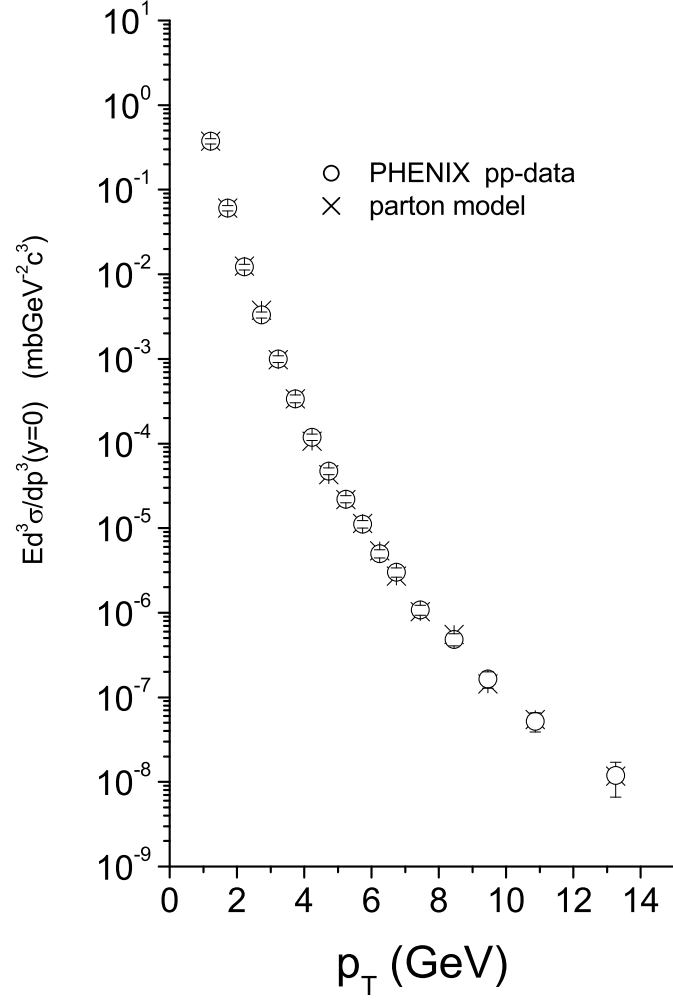


Figure 6: The $pp \rightarrow \pi^0 + X$ differential cross section for the PHENIX experiment ($\sqrt{s} = 200 \text{ GeV}$). The experimental data are presented by open circles while the crosses indicate the parton model calculation using a non-Gaussian k_T -smearing. Only the experimental errors can be seen at this scale.

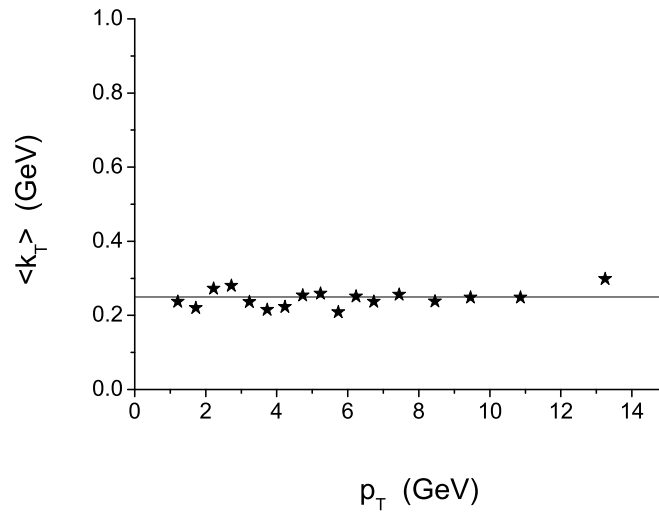


Figure 7: The function $\langle k_T(p_T) \rangle$ obtained using the non-Gaussian $g(\vec{k}_T)$ in the parton model description of the PHENIX data. The solid line at 250 *MeV* is shown as a guide.